

# Devulcanization of Waste Rubber and Generation of Active Sites for Silica Reinforcement

Soumyajit Ghorai,<sup>†</sup> Dipankar Mondal,<sup>‡</sup> Sakrit Hait,<sup>§</sup> Anik Kumar Ghosh,<sup>§</sup> Sven Wiessner,<sup>§</sup> Amit Das,<sup>\*,§</sup> and Debapriya De<sup>\*,†</sup>

<sup>†</sup>Chemistry Department, MCKV Institute of Engineering, Liluah, Howrah 711204, India

<sup>‡</sup>Department of Polymer Science and Technology, University of Calcutta, Kolkata 700009, India

<sup>§</sup>Leibniz-Institut für Polymerforschung Dresden e.V., D-01069 Dresden, Germany

**ABSTRACT:** Each year, hundreds of millions of tires are produced and ultimately disposed into nature. To address this serious environmental issue, devulcanization could be one of the sustainable solutions that still remains as one of the biggest challenges across the globe. In this work, sulfur-vulcanized natural rubber (NR) is mechanochemically devulcanized utilizing a silane-based tetrasulfide as a devulcanizing agent, and subsequently, silica (SiO<sub>2</sub>)-based rubber composites are prepared. This method not only breaks the sulfur–sulfur cross-links but also produces reactive poly(isoprene) chains to interact with silica. The silica natural rubber composites are prepared by replacing 30% fresh NR by devulcanized NR with varying contents of silica. The composites exhibit excellent mechanical properties, tear strength, abrasion resistance, and dynamic mechanical properties as compared with the fresh natural rubber silica composites. The tensile strength of devulcanized rubber-based silica composites is ~20 MPa, and the maximum elongation strain is ~921%. The devulcanized composites are studied in detail by chemical, mechanical, and morphological analyses. Thus, the value added by the devulcanized rubber could attract the attention of recycling community for its sustainable applications.



## INTRODUCTION

About 70% of the rubber grown in the world finds its use in tires. The quantity of waste tires discarded worldwide every year is closely 800 million (10 million tons), and taking into consideration that the amount of natural and synthetic rubber in tires is approximately 60%, about 6 million tons of scrap tires are generated each year. Note that the developed countries have been paying a great deal of attention to the widespread utilization of discarded tires to attain the goals of protecting the environment and recycling resources.<sup>1–3</sup> As a solution to the disposal problem of waste rubber, landfilling, incineration, pyrolysis, and devulcanization/reclaiming of waste rubber products have been proposed. The European Commission forbade the landfilling of end-of-life tires since 1999. Among various techniques, the least enviable disposal is discarding the material. This is a situation that does not add value from the product side, and besides, the value added is negative. Although the threatening pollution problem due to waste tire could be circumvented by using them as a heat source, this is not a favored method from the environmental aspect. For example, when waste rubber products are incinerated, secondary pollutants such as harmful gases and obnoxious smell are produced, which largely pollute air. Moreover, the huge amount of CO<sub>2</sub> generated due to incineration of scrap rubber is also responsible for global warming. Devulcanization/reclaiming of scrap rubber is, therefore, the most advantageous technique to solve the disposal problem. Devulcanization/reclaiming not only pro-

ducts our habitat but also saves our nonrenewable petroleum resources from which the raw material is originated.

Therefore, the most efficient method for disposal of scrap tires is devulcanization/reclaiming, which includes mechanochemical,<sup>4–7</sup> ultrasound,<sup>8–10</sup> microwave,<sup>11–13</sup> or microbial desulfurization technique.<sup>14,15</sup> A good amount of exhaustive information can be gathered on the up-to-date information of rubber devulcanization in different reviews available in the literature.<sup>16–20</sup> Thermomechanical reclaiming of rubber industry wastes was performed in an industrial twin-screw extruder at various barrel temperatures in the range of 80–220 °C.<sup>21</sup> In this process, a high extent of reclaiming (~90%) was achieved. The measurement of swelling values and the corresponding Horikx plot indicated that more selective sulfur bond scission occurred when the sample was treated at 80 and 100 °C. Chemothermomechanical devulcanization of waste rubber powder was performed using 4,4'-dithiobis(2,6-di-*t*-butylphenol) in an internal mixer at 180 and 200 °C.<sup>22</sup> The results suggest that higher temperatures and devulcanizing agent concentrations lower the cross-link density and Mooney viscosity of devulcanized rubber and enhance the sol content of devulcanized rubber. Choline chloride-based deep eutectic solvents (DESSs) such as ChCl:urea, ChCl:ZnCl<sub>2</sub>, and ZnCl<sub>2</sub>:urea are used for devulcanization of ground rubber

Received: May 16, 2019

Accepted: September 4, 2019

Published: October 18, 2019

tire (GTR).<sup>23</sup> Here, GTR are mixed with different DESs followed by ultrasonic (37 kHz) treatment at 180 °C to investigate the extent of devulcanization. It was noticed that a greater extent of devulcanization was obtained at relatively high temperature and mass ratio of rubber to DESs due to the considerable decrease in the cross-link density of the devulcanized GTR. Mechanochemical devulcanization of natural rubber<sup>24</sup> and styrene/butadiene rubber<sup>25</sup> vulcanizates was carried out using different concentrations of bis(3-triethoxysilylpropyl)tetrasulfide at ~70 °C in an open-roll mixing mill. The findings indicated that a higher extent of devulcanization was achieved when the devulcanization time is 40 min and the corresponding devulcanizing agent concentration is 6 phr. Microwave electromagnetic energy was utilized to devulcanize waste tire rubber (WTR) powder with the ultimate goal of producing a composite material by its incorporation in an epoxy resin.<sup>26</sup> The waste tire rubber powder (WTR) and the devulcanized waste tire rubber powder (DWTR) were independently used to grow epoxy resin-based composites, and their performances were evaluated. The results showed that the epoxy composites loaded with DWTR have superior mechanical properties compared to WTR-loaded epoxy composites. Ultrasonically devulcanized (dose, 15 kHz) waste rubber was blended with SBR at various concentrations, and subsequently, the blends were treated with gamma irradiation.<sup>27</sup> The results indicated that the highest compatibility for compounding and revulcanization was observed as compared to the fresh SBR compound. Devulcanization of ground truck tire rubber was performed by supercritical CO<sub>2</sub> in the presence of diphenyl disulfide as the devulcanizing agent.<sup>28</sup> The reaction conditions such as temperature and pressure were maintained at 180 °C and 15 MPa, respectively, and the ratio between the rubber and devulcanizing agent was 1:10. The results show that the treatment in the presence of diphenyl disulfide with supercritical CO<sub>2</sub> decreases the cross-link density of devulcanized rubber and increases the gel fraction and the compatibility of devulcanized rubber with the fresh rubber.

On the other hand, silica is gaining importance in the rubber industry not only for the improvement of the tear strength and abrasion resistance but also for the enhancement of the dynamic mechanical properties such as wet skid resistance and rolling resistance.<sup>29,30</sup> However, incorporation and homogeneous dispersion of silica filler into nonpolar rubbers such as natural rubber (NR), styrene butadiene rubber (SBR), and butadiene rubber (BR) without any compatibilizer are difficult tasks because it arises out of the strong filler–filler interaction and the strong agglomeration tendency of silica particles resulting from the hydrogen bonding and van der Waals forces, leading to the poor compatibility between the silica and rubber matrix. Precisely, these factors restrict the application of silica in different product developments. Furthermore, the –OH groups on the silica surface may constitute hydrogen bonds with the polar groups, present in the accelerator compound, resulting in adsorption of basic accelerators on the acidic surfaces of silica, and thus, the optimum cure time increased.<sup>31</sup> To overcome these difficulties in silica surface modification by different chemicals seems to be a practical and efficient approach. Different organosilanes used to modify silica surface contain hydrolyzable alkoxy groups at one end that can interact with the silanol group on the silica surface, and the hydrophobic group on the other hand can bridge with the rubber chain. Thus, organosilanes can successfully increase the

compatibility of organosilane-modified silica in the rubber matrix and enhance the extent of dispersion.<sup>32–35</sup> The silica surface modification by plasma treatment could improve the dispersion of filler into the rubber matrix and filler–rubber interaction.<sup>36</sup> In this study, the plasma polymerization of acetylene (coating) on silica surface was carried out. The as-grown surface-modified silica was then used as filler in SBR, and hence, its performance was compared with those of the untreated and silane-modified silica composites. The result shows that plasma polymerization and silane modification of silica particles significantly improve their homogeneous dispersion in the SBR matrix. However, SBR vulcanizates having plasma-treated silica show enhancement in tensile strength, improvement in modulus, and acceptable elongation at break. In an alternative approach, functional groups such as hydroxyl groups,<sup>37,38</sup> carboxyl group,<sup>39,40</sup> epoxy groups,<sup>41–43</sup> and alkoxy silane groups<sup>44</sup> provide the rubber matrices as reactive functional sites and make them vulnerable to react with hydroxyl groups of the silica and impart reinforcement into the silica/rubber composite. Among these different types of functionalization, epoxy group has been proven to be the best due to strong silica/rubber interaction.<sup>41–43</sup> The silica surface modification with vulcanization accelerator has opened up new avenues for the development of high-performance rubber composites. Zhong et al.<sup>45</sup> demonstrated the superior mechanical performance of vulcanization accelerator modified silica of styrene butadiene rubber vulcanizates. Here, accelerator ethylenethiourea (ETU) was chemically grafted onto the surface of silane-modified silica to form ETU-modified silica. Owing to uniform dispersion of the ETU-modified silica in the styrene butadiene rubber (SBR) matrix, a strong filler–rubber interaction is observed, and the developed material shows excellent mechanical properties compared to the unmodified silica/SBR composite. The improved rubber–filler interaction in silica/rubber composites is achieved by modification of silica surface with the antioxidant, 2-mercaptobenzimidazole (MB).<sup>46</sup> The developed MB-modified silica/SBR composite exhibits better dispersion and improved mechanical behavior in comparison with the unmodified silica/SBR composite. Chen et al.<sup>47</sup> synthesized silica-supported sulfur monochloride by the chemical interaction between chlorine atom and the silanol hydroxyl group. These functionalized silica nanoparticles can successfully cross-link the rubber chains without sulfur and dramatically enhance the filler–rubber interaction, which significantly improves the dispersion of modified silica in the NR matrix, and thus, enhancement of the mechanical properties occurs. Silanization modification of silica by bis(3-triethoxysilylpropyl)tetrasulfide (TESPT) was carried out using a phosphonium ionic liquid (PIL) catalyst.<sup>48</sup> It was found that phosphonium ionic liquid efficiently catalyzed the silanization reactivity between silica and TESPT in the rubber matrix. The phosphonium ionic liquid reacts with the silanol group on the silica surface to form more nucleophilic silanolate anions, which facilitates the condensation reaction with the ethoxy group in TESPT and increases the degree of silanization. Moreover, morphological and interfacial studies illustrate that the dispersion of silica and interfacial interaction between silica and rubber matrix improved in the SBR/PIL-TESPT-silica composite with respect to the SBR/TESPT-silica composite. SBR/graphene composites having different and tailored surface chemistry were synthesized through in situ chemical reduction of graphene oxide (GO).<sup>49</sup> The results showed that the CO<sub>x</sub>

**Table 1. Compound Formulation of the NR/DeVulcNR/SiO<sub>2</sub> Blend System<sup>a</sup>**

materials (phr)	sample code					
	Silica-10	Silica-20	Silica-30	Silica-40	Silica-30 (control)	Silica-30 (control-TESPT)
NR (RSS 1)	70	70	70	70	100	100
DeVulcNR	30	30	30	30		
silica (Ultrasil VN3)	10	20	30	40	30	30
bis(3-triethoxysilyl propyl) tetrasulfide (TESPT)						1.5

<sup>a</sup>Compound recipes: Zinc oxide, 5 phr; stearic acid, 2 phr; sulphur, 1.8 phr; and CBS, 1.2 phr added in all the formulations.

fraction greater than 0.2 exhibited a strong effect on the dispersion of graphene in the rubber matrix, whereas the CO<sub>x</sub> fraction less than 0.2 exerted a considerable and positive effect on the interfacial interaction. A simple process is developed to grow recyclable, mechanically strong, and macroscopically responsive elastomer vitrimers through exchangeable  $\beta$ -hydroxyl ester bonds into the epoxidized natural rubber-carbon dot interphase<sup>50</sup> and dynamic dual cross-links of boronic ester bonds and Zn<sup>2+</sup> – O coordination into a commercial epoxidized natural rubber.<sup>51</sup> The so-developed material undergoes remarkable improvement of mechanical properties.

In the present work, the devulcanization of the NR (DeVulcNR) vulcanizate and simultaneous modification of the rubber backbone by tetrasulfane are made. The as-grown devulcanized NR is used to prepare the NR/DeVulcNR/SiO<sub>2</sub> vulcanizates that are analyzed by equilibrium swelling experiments, Fourier transform infrared spectroscopy (FTIR), X-ray diffraction (XRD), and differential scanning calorimetric experiments, and the morphology of the composites is evaluated by scanning electron microscopy.

## EXPERIMENTAL SECTION

**Materials.** Natural rubber (NR) (RSS1, Rubber Board, India), bis(3-triethoxysilyl propyl)tetrasulfide (TESPT) used as a devulcanizing agent, zinc oxide (SD Fine Chem., India), stearic acid (Loba Chemie, India), sulfur (SD Fine Chem., India), *N*-cyclohexyl-benzothiazyl-sulfenamide (CBS), and toluene (SD Fine Chem., India) were used without any further purification. The silica used was precipitated silica (Ultrasil VN-3, Evonik Resource Efficiency GmbH, Wesseling, Germany), and its specific surface area was about 200 m<sup>2</sup>/g.

**Preparation of Ground Natural Rubber (GNR).** Ground natural rubber (GNR) was produced from sulfur-cross-linked natural rubber obtained by mixing of natural rubber (100 phr) with ZnO (5 phr), stearic acid (2 phr), CBS (1.2) phr, and sulfur (1.8) phr using a laboratory size two-roll mixing mill at a friction ratio of 1:1.25. The NR compounds were vulcanized at 150 °C for 3.5 min (optimum cure time) and subsequently aged at 70 ± 2 °C for 96 h. The aged cross-linked NR samples were ground in a two-roll mixing mill to produce GNR. The particle size of GNR ranges from 0.5–0.8 mm. The physical properties like sol content, density, and cross-link density of GNR are found to be 6%, 0.936 g/cm<sup>3</sup>, and 1.034 × 10<sup>-3</sup> mol/cm<sup>3</sup>, respectively. The thermogravimetry analysis (TGA) in a nitrogen atmosphere indicates that the rubber hydrocarbon content, oil content, and char residue are 89.7, 2.8, and 5.6%, respectively.

**Preparation of the Devulcanized Natural Rubber (DeVulcNR).** The GNR (100 g) was extensively mixed with the TESPT (6 mL) (devulcanizing agent) and subsequently soaked for 24 h prior to devulcanization and then transferred

to an open-roll mill. Milling was then carried out by an open two-roll mixing mill at a friction ratio of 1:1.25 for 40 min at 70 °C since the devulcanization time and devulcanizing agent concentration were optimized in our previous paper.<sup>24</sup> It is observed that with an increase in devulcanization time, band formation takes place on the roll, and the powder material is converted to a homogeneous elastomeric material.

**Preparation of NR/DeVulcNR/SiO<sub>2</sub> Composites.** Rubber compounds were developed using the formulation presented in Table 1. Mixing of fresh NR and DeVulcNR was done in a fixed ratio of 70:30 (phr:phr), and the compounding additives were added in a laboratory using a two-roll mill of roll size of 3.8 mm × 8.4 mm with a friction ratio of 1:1.25. In such formulations, the compounding additives like zinc oxide, stearic acid, sulfur, and accelerator were added in the proportion based on a total of 100 g of rubber independent of the proportion of DeVulcNR, as it was published by the author<sup>52</sup> that the compounding ingredients in devulcanized rubber derived from the parent compound were inactive. Here, the CBS/semi-EV sulfur vulcanization system is used as the mechanical properties of the CBS/semi-EV system are better compared to those of the EV and the CV systems.<sup>53</sup> To optimize the silica content in the NR/DeVulcNR blend system, varied proportions of silica (10–40 phr) were incorporated into the rubber matrix, and the evaluation of properties mentioned in the subsequent section clearly indicates that the optimum concentration of silica is 30 phr. The effectiveness of DeVulcNR as a compatibilizer is compared with that of the fresh NR/SiO<sub>2</sub> composite both in the presence and absence of TESPT, a well-known silica coupling agent. In the formulations Silica-10–Silica-40, the silica content varies from 10–40 phr; the formulation Silica-30 (control) contains only fresh NR along with silica (30 phr) and the formulation Silica-30 (control-TESPT) contains fresh NR, silica (30 phr), and TESPT (1.5 phr). Initially, NR and DeVulcNR were mixed on the two-roll mill to prepare a compound and masticated thoroughly for 3–4 min. The compounding additives, for example, ZnO and stearic acid, were then added to the rubber compound for 1–2 min. Then, silica was added in three steps (1/3 silica) in a period of 7–8 min to the rubber compound and mixed thoroughly, and after complete addition of silica, the material was thoroughly mixed for 2 min. Then, sulfur was added to it, followed by the addition of CBS. In the case of the silica (control-TESPT) compound, silica was added along with TESPT in three steps (1/3 silica and 1/3 TESPT) in a period of 7–8 min to the rubber compound.

The curing parameters of the compounds were measured by the Elastograph 67.12 (Göttfert, Germany) at 150 °C. The samples were then cured in press at 150 °C, and 34 MPa pressure for the respective optimum cure time ( $t = t_{90}$ ) was

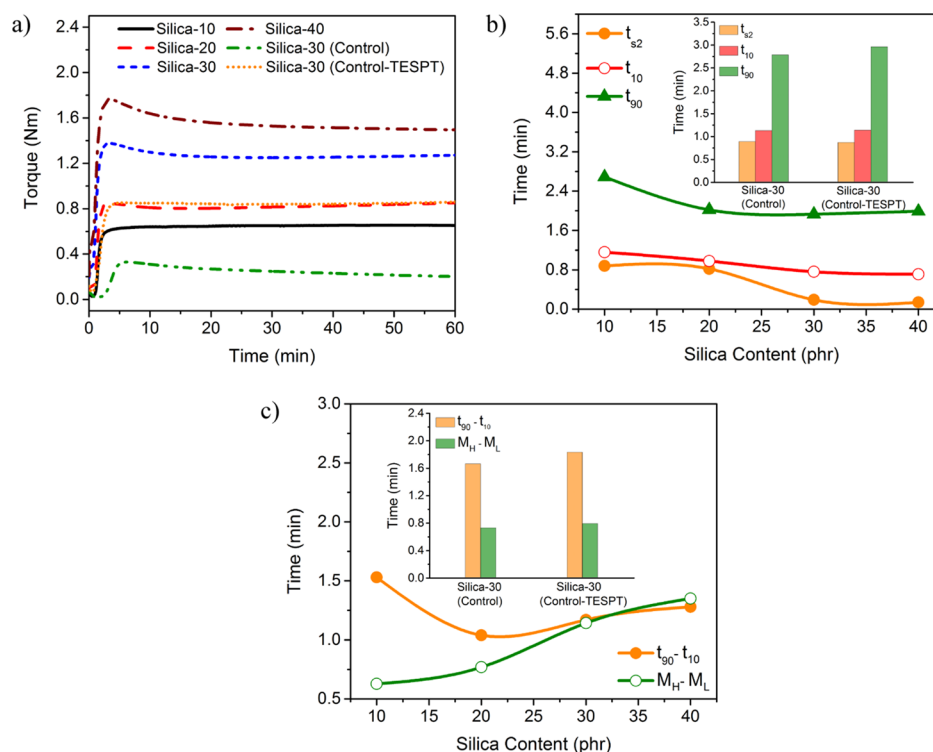


**Figure 1.** Effect of silica content on (a) curing characteristics (b)  $t_{s2}$ ,  $t_{10}$ , and  $t_{90}$  (c) cure rates ( $t_{90} - t_{10}$ ) and extent of cure ( $M_H - M_L$ ) of NR/DeVulcNR/SiO<sub>2</sub>, NR/SiO<sub>2</sub>, and NR/SiO<sub>2</sub>-TESPT systems.

noted from rheograms. The cure rate index (CRI) of the compounds was calculated from the equation as follows

$$\text{CRI} = \frac{100}{t_{90} - t_{s2}} \quad (1)$$

## CHARACTERIZATION

The Fourier transform infrared (FTIR) spectra of the vulcanizates were obtained in the ATR mode using a Bruker, GmbH (model: ALPHA), FTIR spectrophotometer.

Equilibrium swelling measurements of the cured rubber samples were obtained using toluene at room temperature (25°C) as per ASTM D471-16a. The equilibrium swelling value was used to evaluate the average molecular weight between cross-links  $M_c$  by applying the Flory–Rehner equation<sup>54</sup> as follows

$$\nu_c = \frac{1}{M_c} = \frac{\ln(1 - V_{rf}) + V_{rf} + \chi V_{rf}}{V_s d_r \left( V_{rf}^{1/3} - \frac{V_{rf}}{2} \right)} \quad (2)$$

where  $V_{rf}$  is the volume fraction of NR/DeVulcNR vulcanizates in the swollen specimen,  $V_s$  is the molar volume of the solvent (for toluene,  $V_s = 106.2 \text{ cm}^3/\text{mol}$ ),  $d_r$  is the density of rubber vulcanizates, and  $\chi$  is the interaction parameter (for NR/toluene system,  $\chi = 0.393$ ).

The rubber–filler interaction was measured using the Kraus<sup>55</sup> equation as follows

$$\frac{V_{r0}}{V_{rf}} = 1 - m \left[ \frac{f}{1 - f} \right] \quad (3)$$

where  $V_{r0}$  is the volume fraction of the gum vulcanizates,  $f$  is the volume fraction of filler obtained from the ratio of volume

of filler and the total volume of the recipe, and  $m$  is the rubber–filler interaction parameter. The volume fraction ( $V_{rf}$ ) of rubber network in the swollen phase was calculated from the equation of Ellis and Welding.<sup>56</sup>

The degree of reinforcement was evaluated from the Cunneen and Russell<sup>57</sup> equation as follows

$$\frac{V_{r0}}{V_{rf}} = a e^{-z} + b \quad (4)$$

where  $V_{r0}$  and  $V_{rf}$  are the same as defined earlier,  $z$  is the weight fraction of filler, and  $a$  and  $b$  are constants.

Tensile and tear strengths of the composites were evaluated by a universal tensile machine (DigiUTM-2000 V) as per ASTM D 412 and ASTM D 624, respectively. The abrasion resistance of the composites was measured using a DIN abrasion tester following ASTM D 5963.

To get an idea about the dispersion of silica in NR/DeVulcNR/SiO<sub>2</sub> composites, a scanning electron microscopy (SEM) study of the tensile fractured surface was performed on Zeiss EVO-MA10 at 0° tilt angle. The surface of the sample was coated by gold using a sputtering technique.

The calorimetric glass temperature ( $T_g$ ) was determined using differential scanning calorimetry (DSC). Measurements were done in the temperature range of  $-100$  to  $25$  °C, in a nitrogen atmosphere (purge) using a DSC apparatus (model: Netzsch, Germany, model no. 204 F1).

The dynamic mechanical characteristics such as storage modulus ( $E'$ ) and loss tangent ( $\tan \delta$ ) of NR/DeVulcNR/SiO<sub>2</sub> composites were measured using Eplexor 2000 N (Gabo Qualimeter, Ahlden, Germany) at a frequency of 10 Hz. The sample was tested in the temperature range from  $-100$  to  $100$  °C with a heating rate of  $10$  °C/min. The samples were

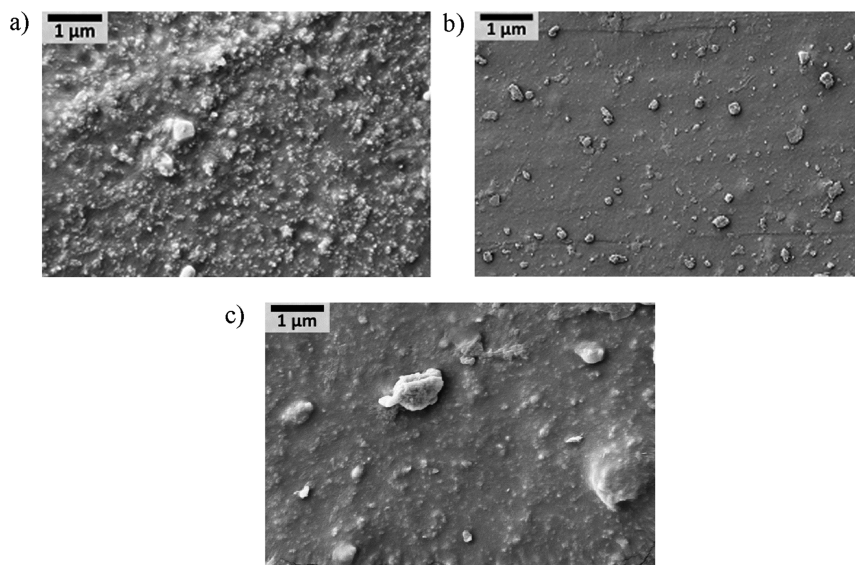


**Figure 2.** SEM photographs of (a) devulcanized Silica-30, (b) Silica-30 with fresh NR and without silane, and (c) Silica-30 with fresh NR and silane.

analyzed in the tension mode with 1% static pre-strain and 0.5% oscillating dynamic strain.

Wide angle X-ray diffraction (WAXD) analysis of the composites was done in an X'Pert-Pro, Pan Analytical diffractometer using  $\text{CuK}\alpha$  ( $\lambda = 1.540$  nm) radiation at a generator voltage of 40 kV and a current of 30 mA with a scanning rate of  $1^\circ/\text{min}$  at room temperature in  $2\theta = 5$  to  $90^\circ$ .

## RESULTS AND DISCUSSION

**Curing Characteristics.** Figure 1a shows rheograms obtained on the elastograph, which indicate the cure behavior of all the compounds. From Figure 1b, we find that with increasing silica loading, both the scorch time ( $t_s$ ) and the optimum cure time ( $t_{90}$ ) of the NR/DeVulcNR/SiO<sub>2</sub> compound show a gradual decrease with the increase in silica content. The decreases in optimum cure time ( $t_{90}$ ) and scorch time ( $t_s$ ) with silica loading may be due to the thermal history of the compounds. During mixing, the increasing silica loading significantly increases the compound viscosity and thus increases the mixing temperature. As in the present study, curatives are added into the rubber just after silica loading; therefore, the compounds with high silica loading are subjected to higher temperature during mixing than the compounds with low silica loading. Thus, both  $t_{90}$  and  $t_s$  decrease with the increase in silica loading. Since the evaluation of the overall mechanical performance of the NR/DeVulcNR/SiO<sub>2</sub> compound indicates that the optimum concentration of silica is 30 phr, therefore, it is compared with that of the NR/SiO<sub>2</sub> and the NR/SiO<sub>2</sub>/TESPT systems with same silica loading (30 phr). The results show that both of the  $t_s$  and  $t_{90}$  of the NR/SiO<sub>2</sub> are much higher compared to those of either the NR/DeVulcNR/SiO<sub>2</sub> or NR/SiO<sub>2</sub>/TESPT compound. This is probably due to less accelerator molecules adsorbed by the silanol groups when the blend system contains DeVulcNR or TESPT as a compatibilizer. The NR/SiO<sub>2</sub>/TESPT compound shows higher  $t_{10}$  and  $t_{90}$  than NR/DeVulcNR/SiO<sub>2</sub>, as shown in Figure 1b. This may be attributed to the stronger interfacial adhesion between SiO<sub>2</sub>-TESPT and NR, leading to more pronounced confinement of NR chains, which in turn, slows

down the vulcanization as compared to that in the NR/DeVulcNR/SiO<sub>2</sub> compound. The difference between  $t_{90}$  and  $t_{10}$ , ( $t_{90} - t_{10}$ ) as presented in Figure 1c is used to determine the vulcanization rate, where a higher vulcanization rate indicates lower ( $t_{90} - t_{10}$ ). From the result, it is evident that the ( $t_{90} - t_{10}$ ) of NR/DeVulcNR/SiO<sub>2</sub> is lower compared to that of NR/SiO<sub>2</sub>/TESPT, which is further lower than that of the NR/SiO<sub>2</sub> for a 30 phr silica loading in all the rubber compounds. The DeVulcNR containing the pendent ethoxy group modifies the silica surface by chemical interaction with the silanol groups on the silica surfaces, decreases the tendency of adsorption of accelerator compounds on silica surfaces, and consequently increases the vulcanization rate. The extent of cure ( $M_H - M_L$ ) increases with an increase in silica loading. The extent of cure is noticed to increase continuously with the increase in silica loading, as presented in Figure 1c. This is due to the fact that the chemical interaction between DeVulcNR containing pendent ethoxy groups with silanol groups on the silica surface could result to additional cross-links in the DeVulcNR phase showing an overall increase in the cross-link density of the vulcanizates. The different NR/DeVulcNR/SiO<sub>2</sub> compounds containing DeVulcNR as an interfacial modifier show a higher extent of cure than the TESPT-containing system at a fixed proportion of silica loading, exhibiting the improvement of filler–rubber interaction in NR/DeVulcNR/SiO<sub>2</sub> composites.

**SEM Failure Surface Morphology.** The homogeneity of NR/DeVulcNR/SiO<sub>2</sub> composites was examined by the scanning electron microscopy analyses of the tensile fractured surface of their vulcanizates. Furthermore, for comparison, other control samples with fresh NR and silica composites are examined. Those images are presented in Figure 2a–c. From Figure 2a, it is observed that the devulcanized sample shows homogeneous and uniform dispersion of silica, and a very fine structure of the silica particles can be obtained at the submicron length scale. However, a few bigger agglomerated structures can also be noticed. In the case of fresh NR silica composites (Figure 2b), the fractured surface is found to be smooth with some bigger aggregated particles embedded on top of the surface. After the addition of silane (Figure 2c) to

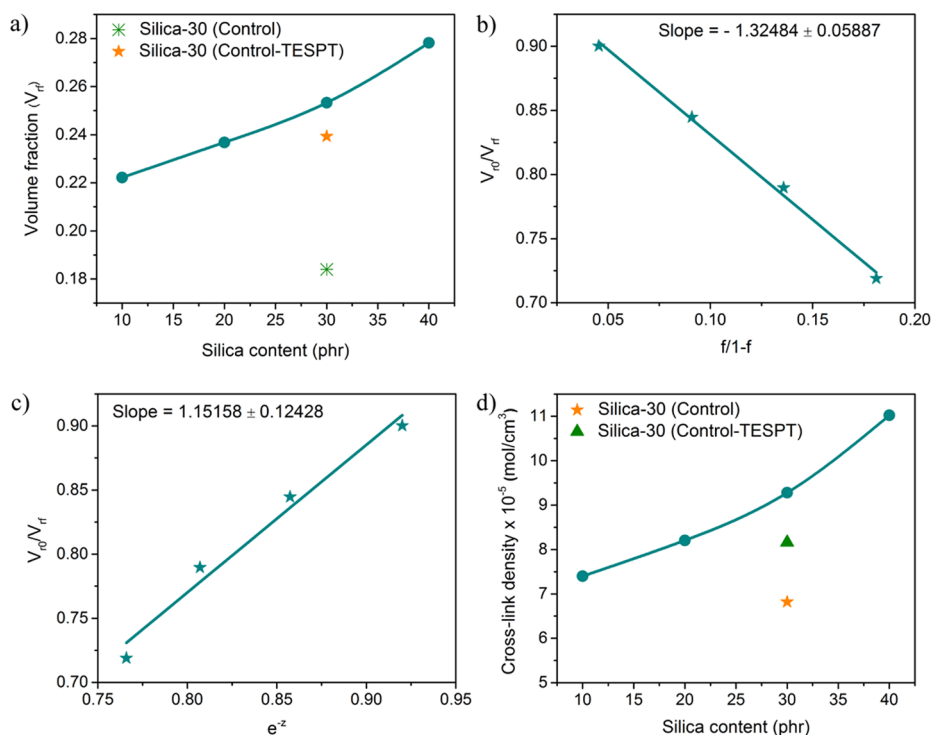


**Figure 3.** (a) Effect of silica content on volume fraction ( $V_r$ ). (b) Variation of  $V_0/V_r$  with  $f/1-f$  (Kraus plot). (c) Variation of  $V_0/V_r$  with  $e^{-z}$  (Cunneen and Russel plot). (d) Effect of silica content on cross-link density of silica rubber composites.

the fresh rubber compounds, the particles are found to be coated by a thin layer of rubber. This finding is associated with the coupling activity of the silane used in the compounds.

**Equilibrium Swelling Measurements.** The rubber–filler interaction of the composites is studied through equilibrium swelling measurement. The volume fraction ( $V_{rf}$ ) of the rubber in swollen composites with silica loading as shown in Figure 3a indicates that with the increase in silica loading, the solvent uptake of the composite decreased, resulting in an increase in volume fraction. Moreover, at a particular concentration of the silica loading (30 phr), the highest rubber–filler interaction is attained for the Silica-30 composite containing DeVulcNR, followed by Silica-30 (control-TESPT) and then Silica-30 (control). The stronger rubber–filler interaction between silica and DeVulcNR can be explained by the formation of chemical linkages between the pendent ethoxy ( $-\text{OC}_2\text{H}_5$ ) groups of DeVulcNR with the silanol ( $-\text{OH}$ ) groups of silica. The reinforcing efficiency of the filler is also determined from the Kraus equation<sup>55</sup> in which a plot of  $\frac{V_0}{V_{rf}}$  versus  $\frac{f}{1-f}$  should give a

straight line. The slope of the straight line could be a measure of the reinforcing capability of the filler. The higher the reinforcing capability of the filler, the higher will be the swelling resistance of the composite because of the presence of filler. The plot of the Kraus equation of NR/DeVulcNR/SiO<sub>2</sub> composites with different proportions of silica loading is shown in Figure 3b. The negative slope of the straight line indicates the reinforcement of the composite. The plot of  $\frac{V_0}{V_{rf}}$  versus  $e^{-z}$

from the Cunneen and Russell relation provides a straight line with a positive slope construed as a measure of the reinforcement behavior of the composites by the filler. The plot of the Cunneen and Russell equation is shown in Figure 3c. The high value of “a” and low value of “b” indicate the

rubber–filler attachment, and  $\frac{V_0}{V_{rf}} < 1$  shows reinforcement.

Therefore, the Kraus and Cunneen and Russell plots indicate the reinforcement of SiO<sub>2</sub> in the NR/DeVulcNR/SiO<sub>2</sub> composites. Furthermore, the increase in the network density with filler contents as evident from Figure 3d may be due to the formation of network structure to the filler surface and subsequently increases the filler–rubber interaction.

The XRD patterns of SiO<sub>2</sub>, Silica-30, and Silica-30 (control) are presented in Figure 4. The broad peak of silica at  $2\theta$  of 23.2° characterizes the noncrystalline structure of silica. Although, in the present case, amorphous precipitated silica

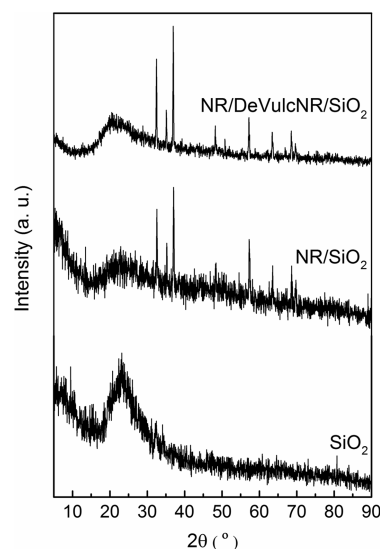


**Figure 4.** XRD patterns of SiO<sub>2</sub>, NR/SiO<sub>2</sub>, and NR/DeVulcNR/SiO<sub>2</sub>.

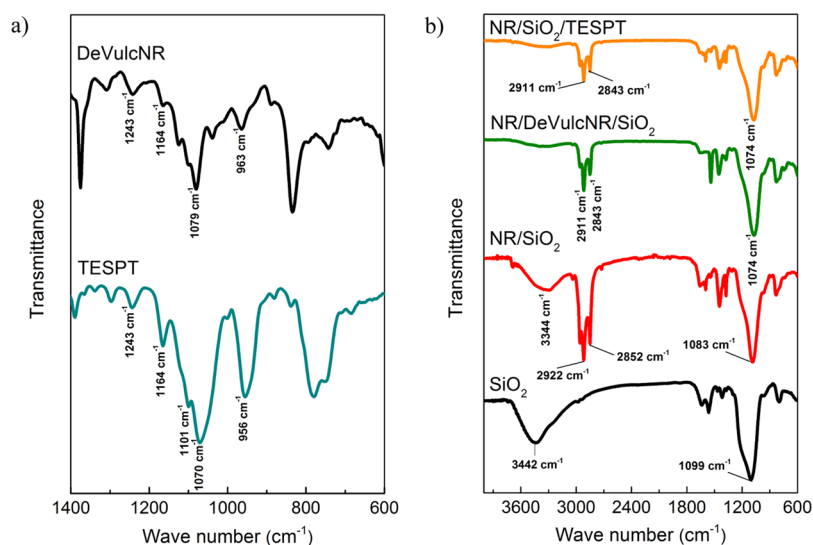


**Figure 5.** (a) FTIR spectra of TESPT and DeVulcNR; (b) FTIR spectra of SiO<sub>2</sub>, NR/SiO<sub>2</sub>, NR/DeVulcNR/SiO<sub>2</sub>, and NR/SiO<sub>2</sub>/TESPT.

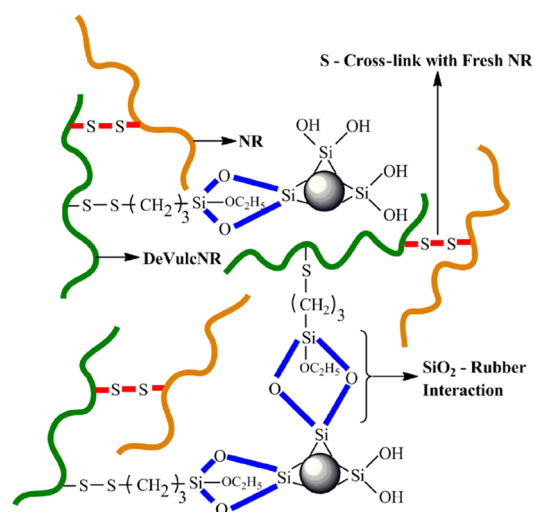
is used, some crystals of silica can be present as impurities. Nevertheless, the peak of silica in the Silica-30 (control) composite appears exactly in the same  $2\theta$  at  $23.2^\circ$ , whereas in the Silica-30 composite with DeVulcNR, the peak shifts from  $23.2$  to  $20.6^\circ$ , which indicates the chemical interaction between SiO<sub>2</sub> and DeVulcNR of the composite on the interface.<sup>43</sup> When silica is added with NR/DeVulcNR, its amorphous structure would change arising out of the chemical bond formation and hydrogen bond interaction<sup>58,59</sup> between Si–OH and pendent ethoxy group (–OEt) of DeVulcNR so that shifting of the diffraction peak of SiO<sub>2</sub> takes place.

**FTIR Analysis.** FTIR analysis is carried out to see the formation of pendent ethoxy-functionalized DeVulcNR and its subsequent reinforcement with silica in the composite. The FTIR spectra of TESPT and DeVulcNR are shown in Figure 5a. The characteristic peaks of TESPT appear at  $1164\text{ cm}^{-1}$  (Si–O cage-like stretching mode),  $1070$  and  $956\text{ cm}^{-1}$  (Si–O stretching), and  $1243\text{ cm}^{-1}$  (symmetric Si–C–H bending). The absorption peaks at  $1164\text{ cm}^{-1}$  for the Si–O cage-like stretching mode,  $1079$  and  $963\text{ cm}^{-1}$  for Si–O stretching, and  $1243\text{ cm}^{-1}$  for symmetric Si–C–H bending also appear in DeVulcNR indicating the presence of fragmented TESPT in DeVulcNR. To gather an idea about the silica reinforcement mechanism of NR/DeVulcNR/SiO<sub>2</sub> composites, FTIR spectra of SiO<sub>2</sub>, NR/SiO<sub>2</sub>, NR/DeVulcNR/SiO<sub>2</sub>, and NR/SiO<sub>2</sub>/TESPT are shown in Figure 5b. The broad peak at  $3442\text{ cm}^{-1}$  corresponds to –OH stretching of Si–OH, and another peak at  $1099\text{ cm}^{-1}$  is attributed to Si–O–Si stretching in silica, whereas –OH stretching appears at  $3344\text{ cm}^{-1}$  and Si–O–Si stretching appears at  $1083\text{ cm}^{-1}$  in NR/SiO<sub>2</sub>. However, no such peak of –OH stretching appears in NR/DeVulcNR/SiO<sub>2</sub> and NR/SiO<sub>2</sub>/TESPT composites, and only the characteristic peak at  $1074\text{ cm}^{-1}$  appears because Si–O–Si stretching emerges.

Thus, it is apparent that the silica reinforcement of the NR/DeVulcNR/SiO<sub>2</sub> composite occurs due to the formation of –Si–O–Si– linkages through chemical reaction between silanol groups present in the silica surface and the pendent ethoxy group of the DeVulcNR or TESPT, as shown in Scheme 1. Moreover, both the DeVulcNR- and TESPT-containing NR/SiO<sub>2</sub> composites show a C–H stretching

vibration of –CH<sub>2</sub>– groups in the rubber backbone at  $2911$  and  $2843\text{ cm}^{-1}$ .

#### Scheme 1. Schematic Presentation of SiO<sub>2</sub> Reinforcement with NR via Interfacial Modifier, DeVulcNR



**Mechanical Properties.** The enhanced rubber–filler interaction along with improved dispersion of silica in the NR/DeVulcNR compound has a considerable influence on the mechanical performance of the composite. The stress–strain behavior of the different composites is shown in Figure 6a. The stress–strain curve distinctly exhibits that the moduli at different % elongation increase with the silica loading in the case of the NR/DeVulcNR/SiO<sub>2</sub> composite. However, the respective values are much inferior for the NR/SiO<sub>2</sub> composite, but the values for Silica-30 and Silica-30 (control-TESPT) are almost comparable. From the Figure 6b, it can be noticed that in the case of NR/DeVulcNR/SiO<sub>2</sub> vulcanizates, stress at 100 and 200% elongation increases with the increase in silica loading up to formulation Silica-40. Tensile strength also enhances with the increase in silica loading up to 30 phr, but with a further increase in silica loading (40 phr), the tensile strength slightly decreases, as presented in Figure 6c.

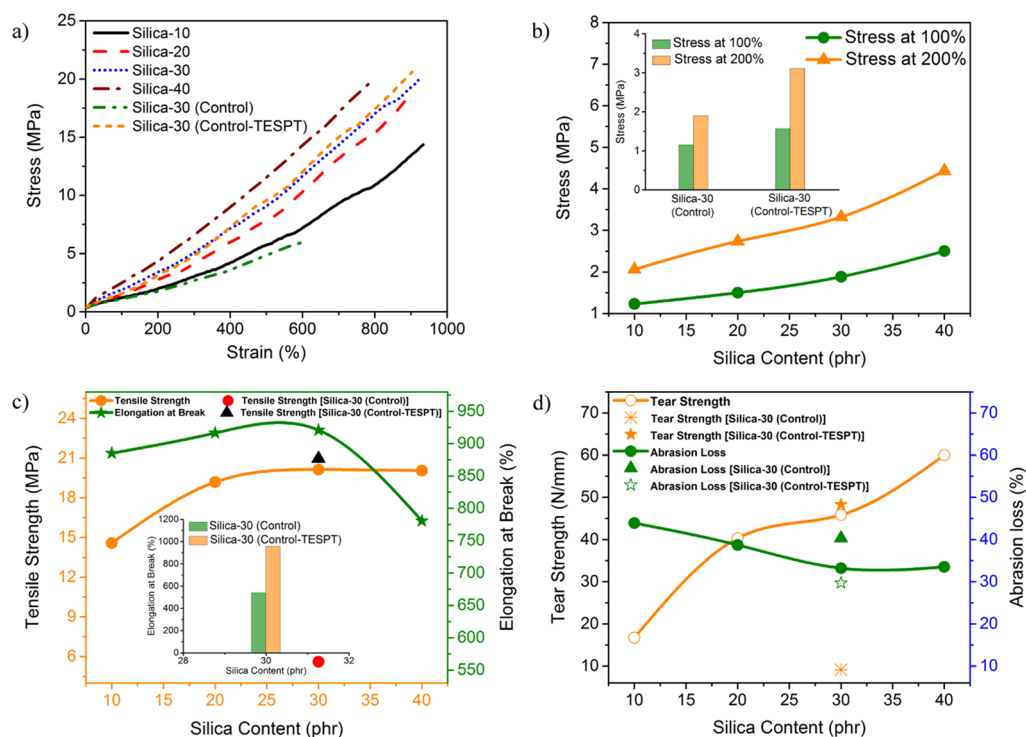


**Figure 6.** (a) Stress–strain behavior of different silica–rubber composites. Effect of (b) stress at 50 and 100% elongation. (c) Tensile strength and elongation at break. (d) Tear strength and abrasion loss with silica content in the composite.

This is due to the fact that with a greater proportion of silica loading, the vulcanizates become stiff and inhibit the stress transmission. The increase in tensile strength of NR/DeVulcNR/SiO<sub>2</sub> composites as compared to the NR/SiO<sub>2</sub> composites clearly indicates the reinforcement of silica filler in which DeVulcNR acts as an interfacial modifier. The pendent ethoxy group present in DeVulcNR eases the dispersion of silica filler through the chemical reaction with the silanol groups present in the silica surface and it shows superior rubber–filler interaction rather than filler–filler interaction. The very high elongation at break of NR/DeVulcNR/SiO<sub>2</sub> vulcanizates is due to the superior interfacial interaction between silica and rubber. Moreover, the elongation at break (Figure 6c) also increased with a silica loading up to 30 phr, which indicates better chain mobility due to silica reinforcement. However, the further increase in silica loading due to agglomeration of silica results in the vulcanizates becoming stiff. Therefore, the chain mobility as well as the elongation at break decreases. To compare the effectiveness of DeVulcNR as a compatibilizer, NR/SiO<sub>2</sub> vulcanizate is prepared in the presence of TESPT, a universally used coupling agent for silica–filler dispersion into the nonpolar rubber compound. The results indicate that the performances of the Silica-30 composite are comparable with those of the Silica-30 (control-TESPT) composite.

The tear strength and abrasion resistance of the NR/DeVulcNR/SiO<sub>2</sub> vulcanizates at different silica loadings and NR/SiO<sub>2</sub> vulcanizates both in the presence and absence of TESPT are evaluated and presented in Figure 6d. From Figure 6d, it is apparent that the tear strength increases with the increase in silica loading, and the maximum value of the tear strength is achieved for a 40 phr silica loading. The results also indicate that the tear strength of NR/DeVulcNR/SiO<sub>2</sub> vulcanizates is much superior to that of the Silica-30

(control-TESPT) vulcanizates. The abrasion loss presented in Figure 6d also decreases with the silica loading, and the lowest value of abrasion loss is achieved for 30 phr. The superior abrasion loss is obtained for the Silica-30 composite as compared to the Silica-30 (control-TESPT) composite.

**Differential Scanning Calorimetry (DSC) Analysis.** The DSC thermograms of the NR/DeVulcNR/SiO<sub>2</sub> blend vulcanizates at various silica loadings and NR/SiO<sub>2</sub> vulcanizates both with and without TESPT are presented in Figure 7. A single

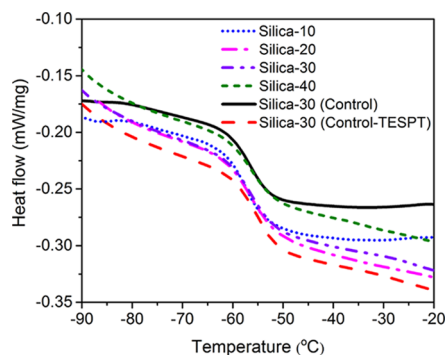


**Figure 7.** DSC thermograms of different silica rubber composites.

glass transition for all the vulcanizates is found in between  $-57.4$  and  $-54.8$  °C. The glass transition temperature and change in the heat capacity and transition width are evaluated from the DSC thermograms and shown in Table 2. The silica content in the NR/DeVulcNR/SiO<sub>2</sub> vulcanizates as well as NR/SiO<sub>2</sub> vulcanizates both with and without TESPT do not show any significant effect on the glass transition temperature ( $T_g$ ). The heat capacity increment ( $\Delta C_p$ ) decreases with increasing silica loading. Since  $\Delta C_p$  is a change in heat capacity of the polymer that participates in glass transition, the decrease

**Table 2.** Parameters Evaluated from DSC Measurements: Onset, Glass Transition, and End Temperature, Heat Capacity Change, and Transition Width of NR/DeVulcNR/SiO<sub>2</sub> Composite

sample code	silica content (phr)	$T_g$ (K)	$\Delta C_p$ (J/(g K))	$\Delta t$ (K)	$\chi_{im}$
Silica-10	10	215.6	0.473	9.7	0.009
Silica-20	20	216.7	0.376	10.0	0.147
Silica-30	30	216.8	0.308	8.5	0.248
Silica-40	40	216.8	0.282	8.8	0.262
Silica-30 (control)	30	218.0	0.527	7.3	0.028
Silica-30 (control-TESPT)	30	218.2	0.303	7.7	0.443

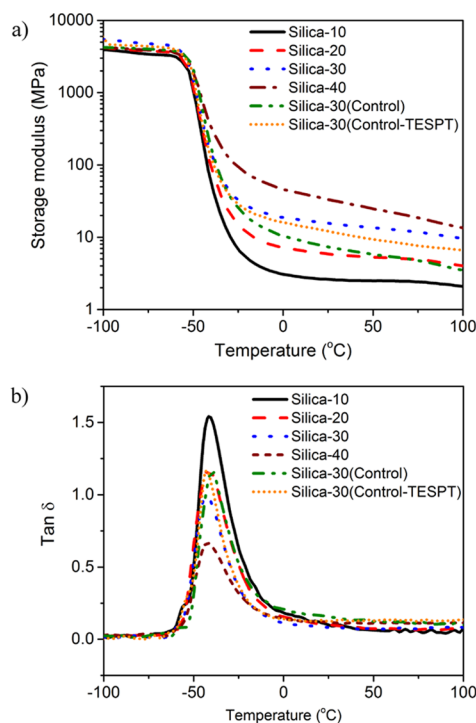
in  $\Delta C_p$  is often studied in terms of an immobilized layer of polymer surrounded with filler particles/crystallites. The fraction of immobilized polymer chain can then be calculated by

$$\chi_{im} = 1 - \frac{\Delta C_p}{\Delta C_p^0(1 - W_{SiO_2})} \quad (5)$$

where  $\Delta C_p^0$  is the change of the heat capacity of the pure rubber and  $W_{SiO_2}$  is the weight fraction of silica, and the values of  $\chi_{im}$  are shown in Table 2. In the case of the NR/DeVulcNR/SiO<sub>2</sub> vulcanizate, the  $\chi_{im}$  value increases with the silica loading. With the increase in silica content, the polymer filler interaction, that is, the reinforcing ability of the vulcanizates increases and so the fraction of immobilized polymer chains increases as well. In the case of the NR/SiO<sub>2</sub> vulcanizates without the coupling agent, the heat capacity increment ( $\Delta C_p$ ) value is much superior compared to that of the others, and consequently, the lowest  $\chi_{im}$  value is obtained, which indicates inferior polymer–filler interaction.

**Dynamic Mechanical Analysis (DMA).** Dynamic mechanical analysis of all the NR/DeVulcNR/SiO<sub>2</sub> composites is studied to have an idea about the silica reinforcement. The temperature dependence of storage modulus ( $E'$ ) and loss factor ( $\tan \delta$ ) of the composites with different silica contents are illustrated in Figure 8a,b and respective data are presented in Table 3.

The storage modulus of the composites can be considered as a direct measure of the filler reinforcement. It is also found to depend on the filler dispersion, rubber–filler interaction, and ultimately the compatibility of the blend.<sup>60,61</sup> As illustrated in Figure 8a and Table 3, it is revealed that the  $E'$  values of NR/DeVulcNR/SiO<sub>2</sub> composites consistently increase with the silica loading, and the highest value is achieved for the 40 phr silica loading. To get an idea about the ability of DeVulcNR as a compatibilizer in NR/DeVulcNR/SiO<sub>2</sub> composites, the  $E'$  values of Silica-30 are compared with those of the Silica-30 (control) and Silica-30 (control-TESPT) composites. The result indicates that in the case of Silica-30 (control) vulcanizates, the room temperature  $E'$  is much poorer due to the incompatibility between the rubber and filler and high filler–filler interaction. The respective value of Silica-30 (control-TESPT) vulcanizates is much higher than that of Silica-30 (control) vulcanizates due to the presence of the coupling agent TESPT that enhances the compatibility between NR and silica and simultaneously increases the rubber–filler interaction. However, the  $E'$  value of Silica-30 (control-TESPT) is almost comparable with that of the Silica-30 due to strong rubber–filler interaction, which is facilitated through the chemical reaction between the pendent ethoxy of DeVulcNR and the hydroxyl group of silica.

**Figure 8.** (a) Storage modulus and (b) loss tangent ( $\tan \delta$ ) of different rubber–SiO<sub>2</sub> composites as a function of temperature.**Table 3.** Dynamic Mechanical Properties of NR/DeVulcNR/SiO<sub>2</sub> Composites

sample code	storage modulus ( $E'$ ) at 25 °C (MPa)	maximum $\tan \delta$	$T_g$ at peak temperature (K)
Silica-10	2.62	1.54	231.4
Silica-20	5.81	1.21	231.3
Silica-30	15.75	1.02	229.8
Silica-40	33.42	0.69	230.4
Silica-30 (control)	7.24	1.17	232.8
Silica-30 (control-TESPT)	12.26	1.17	230.8

The temperature dependence curve (Figure 8b) of the loss factor ( $\tan \delta$ ) indicates that the position of the maximum value of loss tangent ( $\tan \delta_{max}$ ) is not considerably influenced by the silica loading. All the NR/DeVulcNR/SiO<sub>2</sub> composites show the glass transition ( $T_g$ ) in the narrow temperature range from 230 to 233 K, but the highest  $\tan \delta$  at  $T_g$  decreases with silica loading in the NR/DeVulcNR/SiO<sub>2</sub> composite. This could be due to the increasing silica loading, which enhances rubber–filler interaction and consequently hinders the mobility of the rubber chain leading to a rise in  $E'$  and fall in the  $\tan \delta$  value and decreases the viscoelasticity of the

material as well.<sup>62</sup> The SiO<sub>2</sub>–DeVulcNR bonds created during vulcanization improve the rubber–filler interaction.

## CONCLUSIONS

DeVulcNR prepared by mechanochemical devulcanization of vulcanized NR using bis(triethoxysilylpropyl)tetrasulfide is used as an interfacial modifier for NR/DeVulcNR/SiO<sub>2</sub> composites. The improvement in the extent of cure, mechanical, and dynamic mechanical properties of NR/SiO<sub>2</sub> composites in the presence of DeVulcNR can be due to the interaction between the pendent ethoxy functional groups of DeVulcNR and the hydroxyl groups on the silica surface. It can ameliorate the dispersion of silica in the rubber matrix and increase the interfacial interaction between silica and rubber. The silica–rubber interfacial interaction is supported by the XRD analysis, which indicates that the peak shifts from 23.2° in Silica-30 (control) to 20.6° in Silica-30. The FTIR analysis shows the disappearance of –OH stretching of Si–OH at 3344 cm<sup>-1</sup> in Silica-30, which further proves the chemical interaction between silanol groups on the silica surface and ethoxy groups on DeVulcNR. The SEM analysis of Silica-30 shows uniform dispersion of silica at the submicron length scale, whereas in Silica-30 (control), bigger agglomerates appear on top of the surface. The tensile strength and elongation at break of the Silica-30 composite are 20.13 MPa and 921%, respectively, whereas the respective values are 5.61 MPa and 539% respectively. The assessment of the immobilized polymer fraction chains by DSC study shows that with the increase in silica loading, fraction of immobilized polymer chains decreases. The efficiency of DeVulcNR as interfacial modifier in the Silica-30 composites is compared with TESPT, a conventional coupling agent of silica in the Silica-30 (control-TESPT) composites. The properties of both the composites are comparable but greatly superior as compared to Silica-30 (control) composites.

## AUTHOR INFORMATION

### Corresponding Authors

\*E-mail: [das@ipfdd.de](mailto:das@ipfdd.de) (A.D.).

\*E-mail: [d.de@mckvie.edu.in](mailto:d.de@mckvie.edu.in). Phone: 91-033-26549315. Fax: 91-033-26549318 (D.D.).

### ORCID

Amit Das: 0000-0002-2579-1369

### Notes

The authors declare no competing financial interest.

## ACKNOWLEDGMENTS

The financial support by the Department of Science and Technology (DST) and Science and Engineering Research Board (SERB), New Delhi, India, (project no. SB/S3/ME/40/2013 dated April 09, 2014) is thankfully acknowledged for carrying out the research work.

## REFERENCES

- (1) Dobrotă, D.; Dobrotă, G. An innovative method in the regeneration of waste rubber and the sustainable development. *J. Cleaner Prod.* **2018**, *172*, 3591–3599.
- (2) Asaro, L.; Gratton, M.; Seghar, S.; Hocine, N. A. Recycling of rubber wastes by devulcanization. *Resour., Conserv. Recycl.* **2018**, *133*, 250–262.
- (3) Thomas, B. S.; Kumar, S.; Mehra, P.; Gupta, R. C.; Joseph, M.; Csetenyi, L. J. Abrasion resistance of sustainable green concrete

containing waste tire rubber particles. *Constr. Build. Mater.* **2016**, *124*, 906–909.

- (4) De, D.; Das, A.; De, D.; Dey, B.; Debnath, S. C.; Roy, B. C. Reclaiming of ground rubber tire (GRT) by a novel reclaiming agent. *Eur. Polym. J.* **2006**, *42*, 917–927.

- (5) Mohaved, S. O.; Ansarifard, A.; Nezhad, S. K.; Atharyfar, S. A novel industrial technique for recycling ethylene-propylene-diene waste rubber. *Polym. Degrad. Stab.* **2015**, *111*, 114–123.

- (6) De, D.; Maiti, S.; Adhikari, B. Reclaiming of Rubber by a Renewable Resource material (RRM). II. Comparative Evaluation of Reclaiming Process of NR Vulcanizate by RRM and Diallyl disulfide. *J. Appl. Polym. Sci.* **1999**, *73*, 2951–2958.

- (7) Sabzekar, M.; Chenar, M. P.; Mortazavi, S. M.; Kariminejad, M.; Asadi, S.; Zohuri, G. Influence of process variables on chemical devulcanization of sulfur-cured natural rubber. *Polym. Degrad. Stab.* **2015**, *118*, 88–95.

- (8) Maridass, B.; Gupta, B. R. Process optimization of devulcanization of waste rubber powder from syringe stoppers by twin screw extruder using response surface methodology. *Polym. Compos.* **2008**, *29*, 1350–1357.

- (9) Oh, J. S.; Isayev, A. I. Continuous ultrasonic devulcanization of unfilled butadiene rubber. *J. Appl. Polym. Sci.* **2004**, *93*, 1166–1174.

- (10) Feng, W.; Isayev, A. I. Continuous ultrasonic devulcanization of unfilled butyl rubber. *J. Appl. Polym. Sci.* **2004**, *94*, 1316–1325.

- (11) de Sousa, F. D. B.; Scuracchio, C. H.; Hu, G.-H.; Hoppe, S. Devulcanization of waste tire rubber by microwaves. *Polym. Degrad. Stab.* **2017**, *138*, 169–181.

- (12) Pistor, V.; Scuracchio, C. H.; Oliveira, P. J.; Fiorio, R.; Zattera, A. J. Devulcanization of ethylene-propylene-diene polymer residues by microwave—Influence of the presence of paraffinic oil. *Polym. Eng. Sci.* **2011**, *51*, 697–703.

- (13) Zanchet, A.; Carli, L. N.; Giovanela, M.; Brandalise, R. N.; Crespo, J. S. Use of styrene butadiene rubber industrial waste devulcanized by microwave in rubber composites for automotive application. *Mater. Des.* **2012**, *39*, 437–443.

- (14) Yao, C.; Zhao, S.; Wang, Y.; Wang, B.; Wei, M.; Hu, M. Microbial desulfurization of waste latex rubber with *Alicyclobacillus* sp. *Polym. Degrad. Stab.* **2013**, *98*, 1724–1730.

- (15) Li, Y.; Zhao, S.; Wang, Y. Microbial desulfurization of ground tire rubber by *thiobacillus ferrooxidans*. *Polym. Degrad. Stab.* **2011**, *96*, 1662–1668.

- (16) Warner, W. C. Methods of devulcanization. *Rubber Chem. Technol.* **1994**, *67*, 559–566.

- (17) Adhikari, B.; De, D.; Maiti, S. Reclamation and recycling of waste rubber. *Prog. Polym. Sci.* **2000**, *25*, 909–948.

- (18) Rajan, V. V.; Dierkes, W. K.; Joseph, R.; Noordermeer, J. W. M. Science and technology of rubber reclamation with special attention to NR-based waste latex products. *Prog. Polym. Sci.* **2006**, *31*, 811–834.

- (19) Karger-Kocsis, J.; Mészáros, L.; Bárány, T. Ground tyre rubber (GTR) in thermoplastics, thermosets, and rubbers. *J. Mater. Sci.* **2013**, *48*, 1–38.

- (20) Ramarad, S.; Khalid, M.; Ratnam, C. T.; Chuah, A. L.; Rashmi, W. Waste tire rubber in polymer blends: A review on the evolution, properties and future. *Prog. Mater. Sci.* **2015**, *72*, 100–140.

- (21) Seghar, S.; Asaro, L.; Rolland-Monnet, M.; Hocine, N. A. Thermo-mechanical devulcanization and recycling of rubber industry waste. *Resour. Conserv. Recycl.* **2019**, *144*, 180–186.

- (22) Zhang, X.; Saha, P.; Cao, L.; Li, H.; Kim, J. Devulcanization of waste rubber powder using thiobisphenols as novel reclaiming agent. *Waste Manage.* **2018**, *78*, 980–991.

- (23) Saputra, R.; Walvekar, R.; Khalid, M.; Shahbaz, K.; Ramarad, S. Effective Devulcanization of Ground Tire Rubber Using Choline Chloride-Based Deep Eutectic Solvents. *J. Environ. Chem. Eng.* **2019**, *7*, 103151.

- (24) Ghorai, S.; Bhunia, S.; Roy, M.; De, D. Mechanochemical devulcanization of natural rubber vulcanizate by dual function disulfide chemicals. *Polym. Degrad. Stab.* **2016**, *129*, 34–46.

- (25) Ghosh, J.; Ghorai, S.; Bhunia, S.; Roy, M.; De, D. The role of devulcanizing agent for mechanochemical devulcanization of styrene butadiene rubber vulcanizate. *Polym. Eng. Sci.* **2018**, *58*, 74–85.
- (26) Aoudia, K.; Azem, S.; Hocine, A. N.; Gratton, M.; Pettarin, V.; Seghar, S. Recycling of waste tire rubber: Microwave devulcanization and incorporation in a thermoset resin. *Waste Manage.* **2017**, *60*, 471–481.
- (27) Elnaggar, M. Y.; Fathy, S. E.; Amdeha, E.; Hassan, M. M. Impact of gamma irradiation on virgin styrene butadiene rubber blended with ultrasonically devulcanized waste rubber. *Polym. Eng. Sci.* **2019**, *59*, 807–813.
- (28) Mangili, I.; Collina, E.; Anzano, M.; Pitea, D.; Lasagni, M. Characterization and supercritical CO<sub>2</sub> devulcanization of cryo-ground tire rubber: Influence of devulcanization process on reclaimed material. *Polym. Degrad. Stab.* **2014**, *102*, 15–24.
- (29) Peng, Z.; Kong, L. X.; Li, S. D.; Chen, Y.; Huang, M. F. Self-assembled natural rubber/silica nanocomposites; its preparation and characterization. *Compos. Sci. Technol.* **2007**, *67*, 3130–3139.
- (30) Prasertsri, S.; Rattanasom, N. Fumed and precipitated silica reinforced natural rubber composites prepared from latex system: Mechanical and dynamic properties. *Polym. Test.* **2012**, *31*, 593–605.
- (31) Akikusa, T.; Ito, M. Influence of silica on the vulcanization Reaction by Sulfur/CBS in isoprene rubber. *Nippon Gomu Kyokaishi* **2011**, *267*–272.
- (32) Plueddemann, E. P. *Chemistry of Silane Coupling Agents*. Springer: Boston, MA, 1991; p. 31–54.
- (33) Ten Brinke, J. W.; Debnath, S. C.; Reuvekamp, L. A. E. M.; Noordermeer, J. W. M. Mechanistic aspects of the role of coupling agents in silica-rubber composites. *Compos. Sci. Technol.* **2003**, *63*, 1165–1174.
- (34) Li, Y.; Han, B.; Liu, L.; Zhang, F.; Zhang, L.; Wen, S.; Lu, Y.; Yang, H.; Shen, J. Surface modification of silica by two-step method and properties of solution styrene butadiene rubber (SSBR) nanocomposites filled with modified silica. *Compos. Sci. Technol.* **2013**, *88*, 69–75.
- (35) Kapgate, B. P.; Das, C.; Basu, D.; Das, A.; Heinrich, G. Rubber composites based on silane-treated stöber silica and nitrile rubber. *J. Elastomers Plast.* **2015**, *47*, 248–261.
- (36) Mathew, G.; Huh, M.-Y.; Rhee, J. M.; Lee, M.-H.; Nah, C. Improvement of properties of silica-filled styrene-butadiene rubber composites through plasma surface modification of silica. *Polym. Adv. Technol.* **2004**, *15*, 400–408.
- (37) Scholl, T.; Eisele, U.; Trimbach, J.; Kelbch, S. Solution rubber containing hydroxyl groups. U.S. Patent US 6,319,994 B2, November 20, 2001.
- (38) Edwards, D. C.; Sato, K. Interaction of silica with functionalized SBR. *Rubber Chem. Technol.* **1980**, *53*, 66–79.
- (39) Scholl, T.; Trimbach, J. Rubber compound containing solution rubbers which contain carboxyl groups. U.S. Patent US 6,365,668 B1, April 2, 2002.
- (40) Maghami, S.; Dierkes, W. K.; Noordermeer, J. W. M. Functionalized SBRs in silica reinforced tire tread compounds: evidence for interactions between silica filler and zinc oxide. *Rubber Chem. Technol.* **2016**, *89*, 559–572.
- (41) Qiao, H.; Chao, M.; Hui, D.; Liu, J.; Zheng, J.; Lei, W.; Zhou, X.; Wang, R.; Zhang, L. Enhanced interfacial interaction and excellent performance of silica/epoxy group-functionalized styrene-butadiene rubber (SBR) nanocomposites without any coupling agent. *Compos. Part B* **2017**, *114*, 356–364.
- (42) Sengloyuan, K.; Sahakaro, K.; Dierkes, W. K.; Noordermeer, J. W. M. Silica-reinforced tire tread compounds compatibilized by using epoxidized natural rubber. *Eur. Polym. J.* **2014**, *51*, 69–79.
- (43) Xu, T.; Jia, Z.; Luo, Y.; Jia, D.; Peng, Z. Interfacial interaction between the epoxidized natural rubber and silica in natural rubber/silica composites. *Appl. Surf. Sci.* **2015**, *328*, 306–313.
- (44) Liu, X.; Zhao, S.; Zhang, X.; Li, X.; Bai, Y. Preparation, structure, and properties of solution-polymerized styrene-butadiene rubber with functionalized end-groups and its silica-filled composites. *Polymer* **2014**, *55*, 1964–1976.
- (45) Zhong, B.; Jia, Z.; Luo, Y.; Jia, D. A method to improve the mechanical performance of styrene butadiene rubber via vulcanization accelerator modified silica. *Compos. Sci. Technol.* **2015**, *117*, 46–53.
- (46) Zhong, B.; Jia, Z.; Hu, D.; Luo, Y.; Jia, D. Reinforcement and reinforcing mechanism of styrene-butadiene rubber by antioxidant-modified silica. *Compos. Part A* **2015**, *78*, 303–310.
- (47) Chen, L.; Guo, X.; Luo, Y.; Jia, Z.; Bai, J.; Chen, Y.; Jia, D. Effect of novel supported vulcanizing agent on the interfacial interaction and strain-induced crystallization properties of natural rubber nanocomposites. *Polymer* **2018**, *148*, 390–399.
- (48) Tang, Z.; Huang, J.; Wu, X.; Guo, B.; Zhang, L.; Liu, F. Interface engineering toward promoting silanization by ionic liquid for high-performance rubber/silica Composites. *Ind. Eng. Chem. Res.* **2015**, *54*, 10747–10756.
- (49) Tang, Z.; Zhang, L.; Feng, W.; Guo, B.; Liu, F.; Jia, D. Rational design of graphene surface chemistry for High-Performance rubber/graphene composites. *Macromolecules* **2014**, *47*, 8663–8673.
- (50) Tang, Z.; Liu, Y.; Guo, B.; Zhang, L. Malleable, mechanically strong, and adaptive elastomers enabled by interfacial exchangeable bonds. *Macromolecules* **2017**, *50*, 7584–7592.
- (51) Chen, Y.; Tang, Z.; Liu, Y.; Wu, S.; Guo, B. Mechanically robust, self-healable, and reprocessable elastomers enabled by dynamic dual cross-links. *Macromolecules* **2019**, *52*, 3805–3812.
- (52) De, D.; Maiti, S.; Adhikari, B. Reclaiming of rubber by a renewable resource material (RRM). III. evaluation of properties of NR reclaim. *J. Appl. Polym. Sci.* **2000**, *75*, 1493–1502.
- (53) Ghorai, S.; Jalan, A. K.; Roy, M.; Das, A.; De, D. Tuning of accelerator and curing system in devulcanized green natural rubber compounds. *Polym. Test.* **2018**, *69*, 133–145.
- (54) Flory, P. J.; Rehner, J., Jr. Statistical mechanics of cross-linked polymer networks I. Rubberlike elasticity. *J. Chem. Phys.* **1943**, *11*, 512–520.
- (55) Kraus, G. Swelling of filler-reinforced vulcanizates. *J. Appl. Polym. Sci.* **1963**, *7*, 861–871.
- (56) Ellis, B.; Welding, G. N. *Techniques of Polymer Science*; Society of the Chemical Industry: London, 1964.
- (57) Cunneen, J. I.; Russell, R. M. Occurrence and prevention of changes in the chemical structure of natural rubber tire tread vulcanizates during service. *Rubber Chem. Technol.* **1970**, *43*, 1215–1224.
- (58) Cheng, L.; Zheng, L.; Li, G.; Zeng, J.; Yin, Q. Influence of particle surface properties on the dielectric behavior of silica/epoxy nanocomposites. *Phys. B* **2008**, *403*, 2584–2589.
- (59) Lu, S.; Chun, W.; Yu, J.; Yang, X. Preparation and characterization of the mesoporous SiO<sub>2</sub> – TiO<sub>2</sub>/epoxy resin hybrid materials. *J. Appl. Polym. Sci.* **2008**, *109*, 2095–2102.
- (60) Das, A.; Mahaling, R. N.; Stöckelhuber, K. W.; Heinrich, G. Reinforcement and migration of nanoclay in polychloroprene/ethylene–propylene–diene-monomer rubber blends. *Compos. Sci. Technol.* **2011**, *71*, 276–281.
- (61) Rajasekar, R.; Pal, K.; Heinrich, G.; Das, A.; Das, C. K. Development of nitrile butadiene rubber–nanoclay composites with epoxidized natural rubber as compatibilizer. *Mater. Des.* **2009**, *30*, 3839–3845.
- (62) Suresh Kumar, S. M.; Duraibabu, D.; Subramanian, K. Studies on mechanical, thermal and dynamic mechanical properties of untreated (raw) and treated coconut sheath fiber reinforced epoxy composites. *Mater. Des.* **2014**, *59*, 63–69.